

Dose and Airflow Dependence of Benzyl Alcohol Disposition on Skin

MATTHEW A. MILLER, VARSHA BHATT, GERALD B. KASTING

College of Pharmacy, The University of Cincinnati Medical Center, Cincinnati, Ohio

Received 22 April 2005; revised 24 August 2005; accepted 13 September 2005

Published online in Wiley InterScience (www.interscience.wiley.com). DOI 10.1002/jps.20513

ABSTRACT: The penetration of benzyl alcohol (BA) through split-thickness cadaver skin was measured in nonoccluded Franz cells placed in a fume hood. BA, dissolved in a small volume of ethanol and spiked with ^{14}C radiolabel, was applied to skin at nine doses ranging from 0.9 to 10600 $\mu\text{g}/\text{cm}^2$. The percentage of radioactivity penetrated after 24 h increased gradually with dose, ranging from $19.8 \pm 2.9\%$ at the lowest dose to $29.2 \pm 3.0\%$ at the highest. Less than 4% of the radioactivity was retained in the tissue at 24 h; the remainder was considered to be evaporated. These data and those from a previous study were analyzed in terms of a finite dose diffusion/evaporation model. The analysis showed that the increase in BA absorption with dose was consistent with a threefold increase in BA diffusivity in the stratum corneum, as its concentration increased from tracer levels to saturation. The variable diffusivity model was able to describe the combined observations from the two studies to within an rms error of 4.2% of dose. A method of estimating the diffusion model parameters independently of the experiment was found to yield good agreement with the experimentally-derived values at low and moderate doses.

© 2005 Wiley-Liss, Inc. and the American Pharmacists Association J Pharm Sci 95:281–291, 2006

Keywords: mathematical model; skin; permeability; percutaneous; physicochemical; diffusion; disposition; membrane transport; passive diffusion/transport; toxicokinetics

INTRODUCTION

Quantitative dermal risk assessment for volatile chemicals is routinely carried out for cosmetic and personal care products. Fine fragrances employ concentrated solutions of volatile ingredients from natural and synthetic sources in an even more volatile solvent, usually ethanol or phenox-yethanol. The composition of these products is complex.¹ Fragrances are used at lower levels in a wide variety of consumer products. Risk assessment for these products requires a careful study of each component, with top priority often given to fragrances and preservatives.^{2,3} Estimation of the absorbed dose is key to identifying systemic risks, whereas absorption rate and skin concentrations

are important for understanding contact sensitization thresholds.⁴ The objective of the present study is to characterize the skin disposition of a representative fragrance ingredient, benzyl alcohol (BA), in terms of the diffusion model described in the accompanying study.⁵ To do this, we conducted an *in vitro* study to determine the dose dependence of BA absorption following topical application in ethanol and analyzed these data in conjunction with a previous study of BA skin disposition which evaluated the airflow dependence.⁶

MATERIALS AND METHODS

Chemicals

Carbonyl- ^{14}C BA (55 mCi/mmol; 0.1 mCi/mL in ethanol) was purchased from Moravek Biochemicals (Brea, CA). The radiochemical purity was stated by the manufacturer to be 98.3%. Unlabeled BA and calcium-free Dulbecco's phosphate-

Correspondence to: Gerald B. Kasting (Telephone: 513-558-1817; Fax: 513-558-0978; E-mail: Gerald.Kasting@uc.edu)

Journal of Pharmaceutical Sciences, Vol. 95, 281–291 (2006)

© 2005 Wiley-Liss, Inc. and the American Pharmacists Association

buffered saline were purchased from Sigma-Aldrich (St. Louis, MO). Soluene-350[®] was from Perkin-Elmer Biosciences. Ethanol (95%) was from Aaper (Shelbyville, KY).

Dose-Dependence Study

The method has been previously described.⁷ Split-thickness human cadaver skin (~300 μm) was mounted in modified Franz diffusion cells (0.79 cm^2) and placed in thermostatted aluminum blocks maintained at 37°C in a fume hood with a partially drawn sash. Skin was obtained from three donors, with 4–5 replicates per donor at each dose. The receptor solution (magnetically stirred) was Dulbecco's phosphate-buffered saline, pH 7.4, containing 0.02% sodium azide to inhibit microbial growth. The integrity of the tissue was verified using $^3\text{H}_2\text{O}$.⁸ BA doses ranging from 0.9 $\mu\text{g}/\text{cm}^2$ to 10.6 mg/cm^2 dissolved in ethanol were applied to each skin sample. The dose volume was 5 μL for the smaller doses, 10 μL for the 3.24 mg/cm^2 dose, and 20 μL for the 10.6 mg/cm^2 dose. The applied dose appeared to spread rapidly and evenly across the skin surface, which was visually dry within 10–30 s depending on the dose volume. The receptor solution was removed for analysis at 1, 2, 4, 8, 12, and 24 h postdose and replaced with fresh buffer. Following the last receptor collection, the skin samples were removed from the diffusion cells and dissolved in 2 mL of Soluene[®]. All samples were analyzed by liquid scintillation counting (LSC). All data were first averaged by dose for each donor and were then averaged across donors to obtain the reported results.

Airflow-Dependence Study

This study has been previously reported.⁶ The methodology was similar to the dose-dependence study, except that a single dose of 127 $\mu\text{g}/\text{cm}^2$ of BA dissolved in 10 μL of ethanol was applied to the skin samples and a modified top was fitted to the Franz cells. The setup allowed room air to be drawn over the samples at a controlled flow rate. Volatiles were collected in absorbent cartridges at regular intervals and analyzed (along with the receptor solution samples) by LSC following thermal desorption.

Data Analysis

The cumulative absorption and evaporation data from both experiments were analyzed according

to the diffusion model in Reference [5]. Nonlinear regression analysis was performed in Microsoft Excel[®] as described elsewhere.^{7,9} The quantity minimized was the residual sum of squares normalized by the degrees of freedom, or χ_v^2 as defined by Bevington,¹⁰

$$\chi_v^2 = \frac{1}{n-p} \sum_{i=1}^n w_i [y_i(\text{obs}) - y_i(\text{fit})]^2 \quad (1)$$

where n is the number of observations, p is the number of adjustable parameters, w_i is the weight, and the y_i 's are the cumulative percentages of dose absorbed or evaporated for each observation. The dose-dependence fits were constrained to match the estimated evaporation at 24 h (Tab. 2) by including an appropriately weighted evaporation datum at 24 h into the dataset. In order to assess the stability of the model parameters and the importance of the penetration enhancement effect in the dose-dependence study, several variations on the fitting procedure were conducted. These included constant diffusivity (Model 1) versus variable diffusivity (Model 2), separate analyses of the dose- and airflow-dependence data, and a combined analysis. Both equal weighting and $1/y_i^2$ weighting were investigated. Each of these variations encompassed periods of time in which the residual BA in the system fell into the large dose (Case 2) and small dose (Case 1) limits as described in Reference [5]. A small headspace correction was applied to the evaporation data from the airflow-dependence experiment.¹¹ This adjustment allowed the inclusion of two early time evaporation data at low airflows that had been omitted in a previous analysis.⁶ As this correction was of minor consequence for BA, the details will be reserved for a subsequent report. Values of the squared correlation coefficient r^2 were calculated by treating each type of observation (absorption from the dose study, absorption from the airflow study, and evaporation from the airflow study) as a separate data type having its own mean value. Squared deviations of the observed values from these means were then calculated and summed to produce a total sum of squares (SST). The sum of squared residuals (SSR) was calculated by summing the squared differences of these observations from the calculated values, and r^2 followed from $r^2 = 1 - \text{SSR}/\text{SST}$. This procedure resulted in lower r^2 values than those reported in a previous analysis⁶ and gave more meaningful estimates of the fraction of explained variance.

Absorptive and evaporative fluxes were estimated from the cumulative data by a two-point difference method. Values so calculated were plotted at the midpoint of the collection time interval for graphical presentation. This procedure yields approximations to the true flux versus time profiles due to the discrete nature of the data. It did not affect the fitted model parameters since these were determined from the cumulative data rather than from flux.

For the case of constant diffusivity D , the mathematical model⁵ involves four independent, dimensionless parameters (τ , f , β , and χ) and a scaling parameter (h or h^2/D). The former are related to the dimensional model parameters as follows:

$$\tau = Dt/h^2 \quad \text{reduced time} \quad (2)$$

$$f = h_{\text{dep}}/h \quad \text{fractional deposition depth} \quad (3)$$

$$\beta = hC_{\text{sat}}/M_0 \quad \text{membrane capacity/dose ratio} \quad (4)$$

$$\chi = hk_{\text{evap}}\rho/DC_{\text{sat}} \quad \text{volatility parameter} \quad (5)$$

In Equations 2–5, D is the diffusivity of the permeant in the membrane, t is time, h is the membrane thickness, h_{dep} is the thickness of the deposition region in the upper part of the membrane, C_{sat} is the solubility of the permeant in the membrane, M_0 is the dose, k_{evap} is the evaporative mass transfer coefficient, and ρ is the density of the pure liquid (or solid) form of the permeant. Two useful, dose-related parameters can be defined from these variables: a saturation dose, M_{sat} ,

$$M_{\text{sat}} = h_{\text{dep}}C_{\text{sat}} = (f\beta) \cdot M_0 \quad (6)$$

and a “reduced dose,” M_r ,

$$M_r = (f\beta)^{-1} = M_0/M_{\text{sat}} \quad (7)$$

The former is the amount of permeant required to saturate the deposition region and the latter is the (inverse) ratio of this quantity to the applied dose. For values of $M_r \leq 1$ (Case 1), the permeant fully dissolves into the membrane upon dosing, whereas for $M_r > 1$ (Case 2) a liquid (or solid) film of permeant remains on the skin surface. These two cases lead to different solutions to the diffusion equation in the membrane, and to correspondingly different absorption and evaporation profiles. Another important relationship defines the gas

phase mass transfer coefficient for evaporation, k_g :

$$k_{\text{evap}}\rho = k_g \frac{P_{\text{vp}}\text{MW}}{0.76RT} \quad (8)$$

where P_{vp} is the vapor pressure of the permeant, MW is its molecular weight, R is the gas constant, and T is absolute temperature. This equation allows the evaporation rate to be expressed in terms of a number (k_g) that is fundamentally easier to estimate than k_{evap} . The units of all parameters are given in Reference [5] and their values are discussed later.

Consideration of this problem shows that, for the case of constant D , there are only four parameters that can be independently estimated. (This follows since the scaling parameter is incorporated into Equations 2–5). We found it most straightforward to fit the model to experimental data in terms of the dimensional parameters h^2/D , k_g , and M_{sat} , and the dimensionless ratio f . The remaining model parameters can then be calculated from these values and known physical properties of the permeant using Equations 2–8. The parameter k_g is the diffusion model analog of the evaporation rate constant k_1 in a previous analysis,⁶ which was shown to vary linearly with airflow velocity v to within the precision of the experiment. Hence we chose the airflow dependence for k_g to be

$$k_g = k'_g \cdot \left(\frac{v}{42 \text{ mL/min}} \right) \quad (9)$$

where v is airflow in mL/min (airflow-dependence study) and k'_g is a constant of proportionality. An equivalent value of $v = 42$ mL/min was determined for the dose-dependence study (which was performed in a fume hood) by matching the absorption values to those in the airflow-dependence study at a comparable dose. This value was consistent with results from a previous study.⁷ Equation 9 thus leads to the equality $k_g = k'_g$ for the dose-dependence study.

The fractional deposition depth was varied over the range $f = 0.05$ – 0.3 . A broad optimum was found near the value $f = 0.1$, which also resulted in the least systematic variation in the other model parameters when dose data or airflow data were fitted separately. This value was used in all subsequent analyses.

Initial values of the time constant h^2/D were estimated from the dose-dependence data by separately fitting the model at each individual dose. The value of h^2/D was found to decrease

systematically with increasing dose, as had been observed in a similar analysis of ^{14}C -DEET disposition on skin.⁷ Rather than reporting this variation, we developed a sigmoidal expression for a concentration-dependent diffusion coefficient which varied (approximately) from D_0 at low concentrations to D_{sat} at the saturation concentration C_{sat} . The inflection point of the sigmoid curve was designated C_{trans} and the slope factor as m . Thus,

$$D = D_0 + \frac{D_{\text{sat}} - D_0}{1 + \exp[m(1 - C/C_{\text{trans}})]} \quad (10)$$

where $C = C(x)$ is the local concentration of permeant in the membrane. Calculations for which D was taken to be constant were designated as Model 1; those employing Equation 10 were designated Model 2. Equation 10 is one of many possible forms that such a dependence $D = D(C)$ could take. It was not possible to determine a unique, underlying form of $D(C)$ from the analysis; however, it was possible to estimate the range over which D must vary and an approximate concentration at which the variation must occur to provide a quantitative explanation of the dose-dependence results. Equation 10 gave representative results.

RESULTS

Dose-Dependence Study

Table 1 shows the mean absorption for radioactivity associated with ^{14}C -BA as a function of time and applied dose. Flux profiles associated with these data are shown in Figure 1. Maximum absorption rates were reached within the first

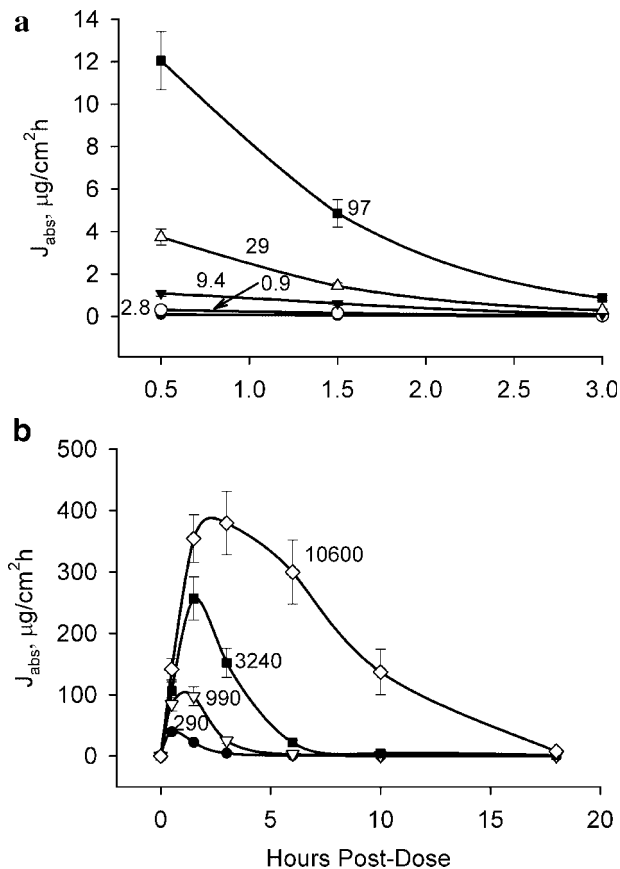


Figure 1. Skin absorption rates for radioactivity associated with ^{14}C -benzyl alcohol (BA) in the dose-dependence study (mean \pm SE of three donors, $n = 4-5$ /donor). The numbers on the graph are the applied dose of BA in $\mu\text{g}/\text{cm}^2$ and the lines are a guide to the eye. (a) Low doses; (b) High doses.

Table 1. Appearance of Radioactivity in the Receptor Solution for Dose-Dependence Skin Disposition Study with ^{14}C -Benzyl Alcohol (BA) (Mean of three Donors, $n = 4-5$ /Donor)

Dose, $\mu\text{g}/\text{cm}^2$	Percentage of Dose					
	0-1 h	1-2 h	2-4 h	4-8 h	8-12 h	12-24 h
0.9	10.2	5.2	2.6	1.1	0.4	0.3
2.8	11.1	5.8	2.5	1.2	0.3	0.2
9.4	11.6	6.5	2.4	0.8	0.3	0.2
29	13.1	5.0	2.0	0.9	0.4	0.4
97	12.4	5.0	1.8	0.5	0.1	0.1
290	13.7	7.7	3.2	1.1	0.3	0.2
990	8.5	9.9	5.0	1.2	0.2	0.2
3240	3.3	7.9	9.4	2.7	0.5	0.4
10600	1.3	3.3	7.2	11.3	5.2	0.9

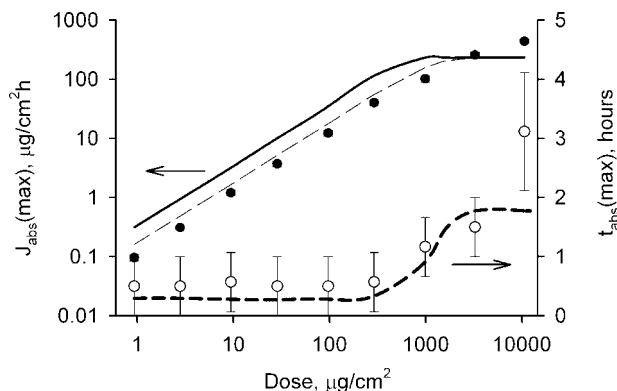


Figure 2. Maximum flux (●) and time-to-maximum flux (○) for absorption of radioactivity in dose-dependence skin disposition study with ^{14}C -BA. The error bars on the closed symbols reflect sample-to-sample variation, whereas those on the open symbols reflect the discrete sampling interval. The curves were calculated from the diffusion model using the bolded parameters in Table 3. Solid line—calculated maximum flux; Light dashed line—apparent maximum flux if measured over experimental sampling interval; Heavy dashed line—time-to-maximum flux.

hour postdose for doses $\leq 300 \mu\text{g}/\text{cm}^2$ and at regularly increasing times for larger doses. This may be clearly seen in the plot of J_{max} and t_{max} shown in Figure 2. Maximum flux (J_{max}) increased with dose at a slightly greater than dose-proportional rate for doses $\leq 300 \mu\text{g}/\text{cm}^2$ and more gradually at larger doses. Consequently, for the smaller doses, the percentages of radioactivity absorbed at any given time increased systematically with dose (Fig. 3). At longer times this trend was continued through the highest dose in the study (Tab. 2). Cumulative absorption ranged from 20% of the applied dose at $0.9 \mu\text{g}/\text{cm}^2$ to 29% at $10600 \mu\text{g}/\text{cm}^2$. Thus, BA increased its own permeation rate through skin under the conditions of the test, that is, it was a mild penetration enhancer.

The amount of radioactivity remaining in the tissue 24 h after application was less than 2% for all doses except the highest, for which 3.8% was retained (Tab. 2). At the lower doses, skin retention was essentially independent of dose, suggesting that the dissipation process was complete by 24 h. Thus, the small amounts of retained ^{14}C appear to be bound to the tissue. Similar results were obtained in the airflow-dependence study.⁶ Further analysis of these data was conducted under the assumption that radioactivity missing from the system at 24 h had evaporated. Evapo-

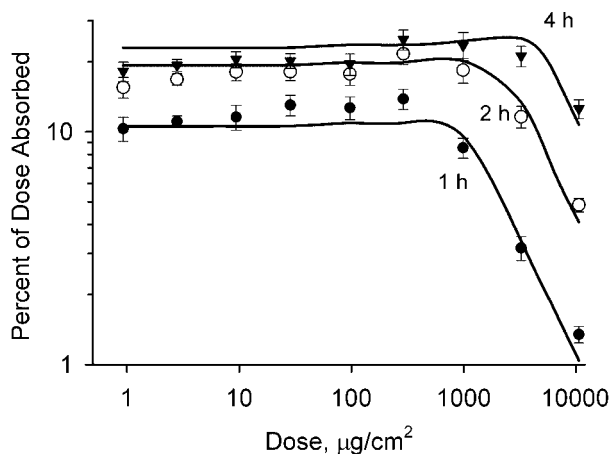


Figure 3. Cumulative percentage of radioactivity in the receptor solutions (mean \pm SE of three donors, $n = 4$ –5/donor) for dose-dependence skin disposition study with ^{14}C -BA. ● 1 h postdose; ○ 2 h postdose; ▼ 4 h postdose. The curves were calculated from the diffusion model using the bolded parameters in Table 3.

ration estimated by this procedure ranged from 67%–79% of the dose (Tab. 2).

Airflow-Dependence Study

These data have been previously reported.⁶ Representative evaporation and absorption rates are shown in Figure 4. The evaporation rate of ^{14}C -BA increased systematically with increasing airflow over the skin surface (Fig. 4a), with a corresponding decrease in the absorption rate (Fig. 4b). The maximum absorption rate occurred within 30 min postdose for airflows of 50–100 mL/min and between 30 and 60 min for airflows of 10–40 mL/min. Maximum evaporation rate occurred within

Table 2. Cumulative Disposition of Radioactivity at 24 h for the Study Reported in Table 1

Dose, $\mu\text{g}/\text{cm}^2$	Absorbed	Skin	Evaporated (Estimated)
0.9	19.8 ± 2.9	1.6 ± 0.1	78.6 ± 3.0
2.8	21.1 ± 1.7	1.0 ± 0.0	77.9 ± 1.7
9.4	21.9 ± 1.1	1.7 ± 0.7	76.4 ± 0.5
29	21.8 ± 0.9	0.6 ± 0.2	77.6 ± 1.1
97	20.0 ± 2.6	0.6 ± 0.0	79.4 ± 2.5
290	26.3 ± 3.2	1.1 ± 0.3	72.6 ± 3.5
990	25.0 ± 4.7	0.6 ± 0.1	74.4 ± 4.8
3240	24.2 ± 3.0	0.7 ± 0.1	75.1 ± 2.9
10600	29.2 ± 3.0	3.8 ± 2.5	67.0 ± 0.6

Results are expressed as percentage of the applied dose (mean \pm SE of three donors).

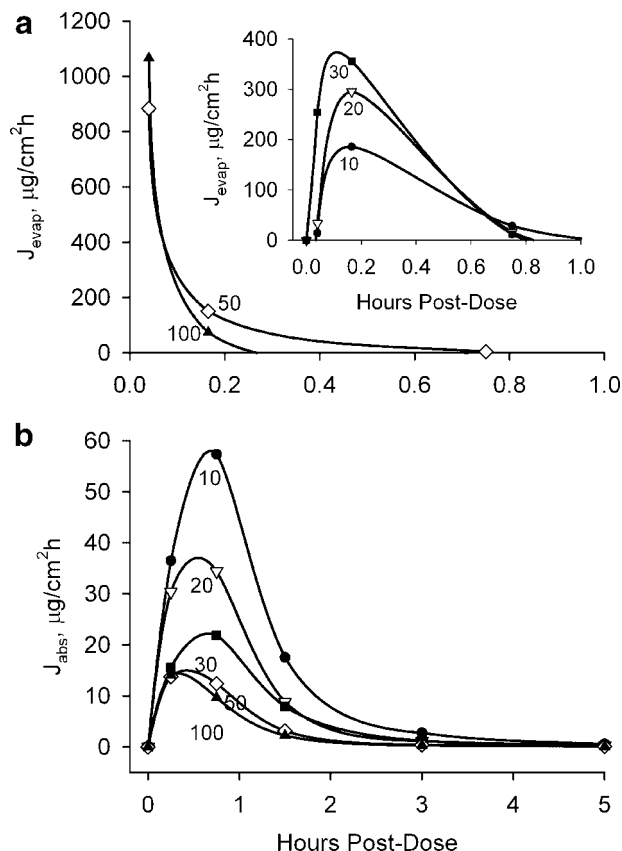


Figure 4. Skin evaporation rates (a) and absorption rates (b) for radioactivity associated with ^{14}C -BA in the airflow-dependence study (mean of two trials).⁶ The numbers on the graph are the airflow over the skin surface in mL/min. The lines are a guide to the eye.

5 min for the higher airflows and between 5 and 15 min for the lower airflows. The delay for the lower airflows is related to the headspace between the skin surface and the vapor trap.^{6,12} These results can be described in terms of compartmental models in which the rate constant for evaporation is proportional to airflow.⁶ No information on skin permeability enhancement was obtained in this study as only a single dose of BA was tested.

Test of Diffusion Model

The diffusion model⁵ was fit to the dose- and airflow-dependence data as described under Methods. The parameters resulting from this process are shown in Table 3. Model calculations are shown in Figures 2, 3, 5, and 6.

For the dose-dependence study, the time constant h^2/D was found to decrease with increasing

dose. The average value of 5.2 h obtained by assuming a constant diffusivity (Model 1) gave a poor representation of the absorption at high doses. This is consistent with the penetration enhancement effect noted earlier (Tab. 2 and Fig. 3) and has also been seen with DEET.⁷ Better fits were obtained using Model 2 in which diffusivity was considered to be a function of the local concentration of BA in the skin. The optimum fit was obtained using a model in which diffusivity increased by a factor of 2.5 as the local BA concentration increased from 0 to its saturation value, C_{sat} . The value of C_{sat} for this fit (calculated from Eq. 6 with $h_{\text{dep}} = 1.5 \mu\text{m}$) was $127 \mu\text{g}/\text{cm}^2 / (1.5 \times 10^{-4} \text{ cm}) \times (\text{mg}/1000 \mu\text{g}) = 850 \text{ mg}/\text{cm}^3$. The degrees of freedom-adjusted residual sum of squares (χ_v^2) was almost fourfold lower with Model 2 than Model 1, an improvement significant at $p < 0.001$.¹⁰ A corresponding increase in the r^2 value of the fit from 0.56 to 0.89 was also obtained.

For the airflow-dependence study, comparable fits were obtained using Models 1 and 2. The optimum values of h^2/D and M_{sat} were lower than those in the dose study by factors of 2 and 3, respectively. When both studies were analyzed together, the airflow study tended to drive the results. This was due in part to the larger number of observations and in part to the fact that the dose study provided no direct data on evaporation. The fit of Model 2 to the combined dataset (bolded values in Tab. 3) was taken to be the best overall representation of the BA disposition data, explaining 94% of the variance in the dataset and yielding an rms deviation of observed and fitted values of 4.2%.

Using the parameters in Table 3, the diffusion model failed to accurately describe the extended "tails" of the evaporation and absorption profiles. Representative comparisons are shown in Figures 5 and 6. Diffusion through a homogeneous membrane with a constant diffusivity leads to terminal exponential behavior of the flux, with the decay constant determined by the leading eigenvalue of the sum of exponentials solution.^{5,13} Thus, such models predict a linear decay of the logarithm of evaporative or absorptive flux with time. Both the dose and airflow studies with BA showed a curvilinear decay (Figs. 5 and 6), indicative of prolonged retention of the radiolabel. Similar behavior has been observed in other studies of fragrance disposition on skin.¹⁴ This phenomenon is a poorly understood aspect of BA disposition in these *in vitro* experiments that is further addressed in the Discussion.

Table 3. Regression Parameters for Diffusion Models of BA Disposition on Skin

Parameters	Units	Dose	Airflow	Combined
Model 1: Constant diffusivity				
h^2/D	h	5.2	2.4	2.2
k'_g	cm/h	1130	930	860
V_h^a	cm ³	[0] ^b	45	42 ^a
M_{sat}	μg/cm ²	142	41	42
v	mL/min	[42]	— ^c	— ^{c,d}
n	—	63	104	167
s	% of dose	4.1	4.1	5.0
r^2	—	0.56	0.95	0.92
χ_v^2	(% of dose) ²	17.1	17.1	24.9
Model 2: Variable diffusivity				
h^2/D_0	h	5.7	2.4	2.6
k'_g	cm/h	1190	1090	880
V_h^a	cm ³	[0]	44	35^a
M_{sat}	μg/cm ²	127	39	34
v	mL/min	42	— ^c	— ^{c,d}
D_{sat}/D_0	—	2.5	[2.5]	3.0
$C_{\text{trans}}/C_{\text{sat}}$	—	0.61	[0.61]	[0.61]
m	—	5.0	[5.0]	[5.0]
n	—	63	104	167
s	% of dose	2.1	4.3	4.2
r^2	—	0.89	0.94	0.94
χ_v^2	(% of dose) ²	4.5	18.6	17.7

A fractional deposition depth $f=0.1$ was used in these analyses.

^a V_h is a headspace volume parameter used to account for the evaporation time lag. The value applies only to data obtained in the airflow-dependence study.

^bBrackets denote parameters that were not optimized for this dataset.

^cValue of v varied systematically from 10–100 mL/min for airflow-dependence study (cf. Reference [6]).

^dValue of v was fixed at 42 mL/min for dose-dependence study.

DISCUSSION

The general features of BA disposition on skin following solvent deposition from ethanol include (1) rapid absorption with peak flux within 1 h except at very large doses (Figs. 1 and 2); (2) evaporation of 45%–85% of the applied dose from the skin surface at rates proportional to airflow over the skin^{6,12} (cf. Tab. 2 and Fig. 4); (3) a 47% increase in percentage absorption at 24 h with dose over the dose range 1–10000 μg/cm² (Tab. 2); and (4) prolonged “tails” to the absorption and evaporation profiles indicative of nonexponential processes (Figs. 5 and 6). The first three of these phenomena were well described by the diffusion model⁵ using a variable diffusivity coefficient that varied by a factor of 2.5–3.0 over the range of estimated concentrations in the skin (Tab. 3, Model 2). The nonexponential behavior was not predicted. *In vivo* studies of other fragrance ingredients^{14,15} and *in vitro* work with DEET^{7,11} suggest that the prolonged release characteristics

of BA from skin under similar test conditions may be shared by other volatile organics. While of little consequence for the cumulative absorption/evaporation ratios, a slow release profile could contribute to prolonged efficacy of either fragrances or insect repellent products.

In order to test whether the prolonged absorption rates were associated with the tissue or with the experimental conditions, we conducted a dose-dependence study for ¹⁴C-BA using a silicone membrane (0.020" or 500 μm) in place of the skin. A constant diffusivity model (Model 1) was then fit to the absorption data using the same procedure as in the skin penetration studies. Representative results are shown in Figure 7. BA penetration through silicone membrane showed even more prolonged absorption rates than had skin, demonstrating that this phenomenon was not associated with the heterogeneous nature of skin or some mysterious “stratum corneum reservoir.” Anissimov and Roberts' analysis¹³ shows that accumulation of solute in the receptor solution can lead

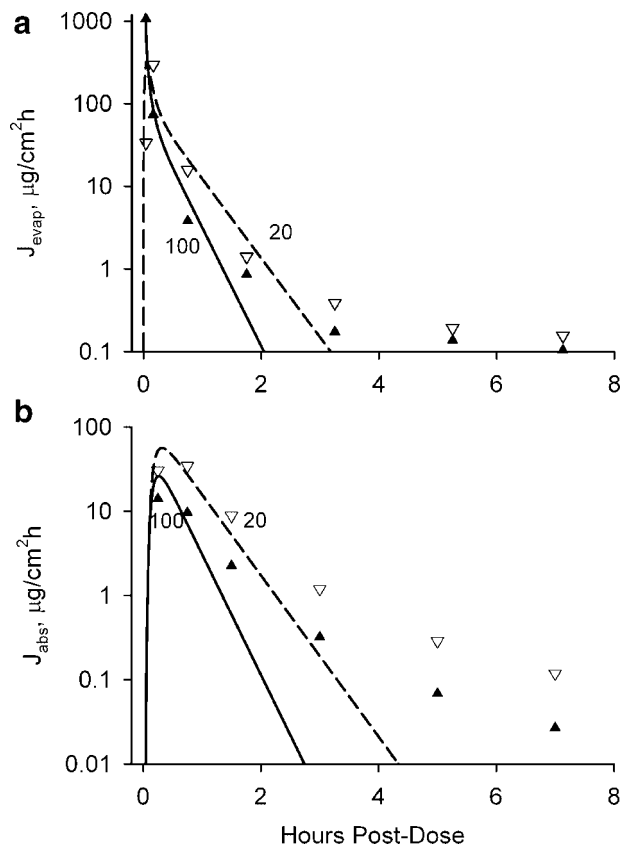


Figure 5. Flux of radioactivity associated with ^{14}C -BA from the surface of the skin in the airflow study. ∇ 20 mL/min; \blacktriangle 100 mL/min (a) evaporation; (b) absorption. The curves are calculations using the bolded parameters in Table 3 (Model 2).

to prolonged flux profiles similar to those in Figures 5b, 6, and 7. However, the receptor solutions were exchanged completely at each sampling point in our studies and the concentration of BA never exceeded 0.6% of its solubility. Therefore, it is unlikely that this feature was associated with a failure to maintain sink conditions. It may be associated with lateral diffusion of radiolabel into the area of the membrane clamped by the ground glass joint, and a corresponding slow release from this region; however, this is still a matter of conjecture. A similar phenomenon could also have occurred in the *in vivo* studies in which a volatiles trap was strapped continuously to the skin.^{12,15} A definitive answer to this question may require an *in vivo* test in which a volatiles trap is applied intermittently rather than continuously. Such experiments require high analytical sensitivity due to the low evaporation rates later in the study.

Other, relatively minor differences between theory and experiment may be understood in

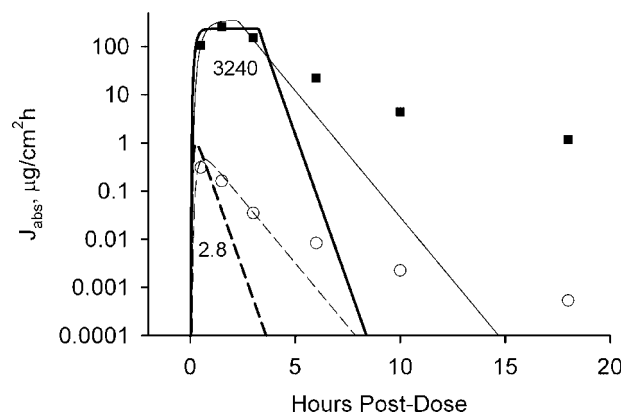


Figure 6. Absorptive flux of radioactivity associated with ^{14}C -BA for the dose-dependence study. \circ 2.8 $\mu\text{g}/\text{cm}^2$; \bullet 3240 $\mu\text{g}/\text{cm}^2$. The heavy lines are calculations using the bolded parameters in Table 3 (Model 2). The thinner lines are calculations using the parameters associated with the fit of Model 2 to the dose data only (Column 3, Tab. 3).

terms of the experimental design. The theory predicts somewhat higher values of the maximum absorptive flux than calculated from the data (Fig. 2); however, the sampling frequency in the experiment lead to averaging of the flux over times comparable to the width of the peak, broadening and lowering the peak shape. When the theoretical flux was averaged over an interval corresponding to the sampling interval (light dashed line in Fig. 2), the agreement between theory and experiment was substantially improved. In any case, this sampling artifact was not a factor in the data

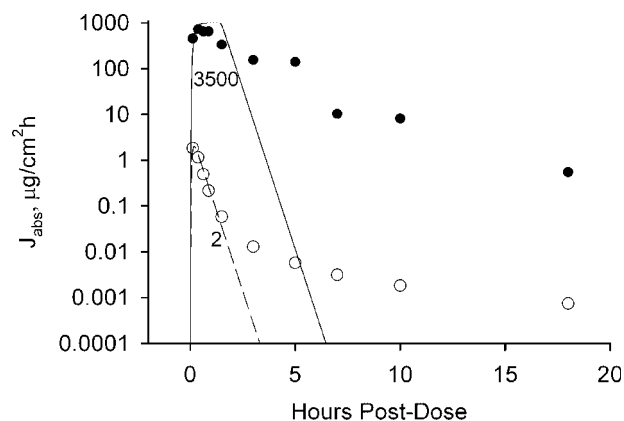


Figure 7. Absorptive flux of radioactivity associated with ^{14}C -BA through silicone rubber membrane (mean of four replicates). \circ 2.0 $\mu\text{g}/\text{cm}^2$; \bullet 3500 $\mu\text{g}/\text{cm}^2$. The lines are calculations based on a fit of Model 1 to the data using the same methods as in the skin absorption studies. The parameter values were $f=0.1$, $h^2/D=1.4$ h, $M_{\text{sat}}=144$ $\mu\text{g}/\text{cm}^2$, and $k'_g=1520$ cm/h.

Table 4. Physical Properties and Auxiliary Skin Permeability Data for BA

Parameter	Units	Value	Reference
Physical and environmental properties			
MW	g/mol	108.1	—
ρ^a	g/cm ³	1.04	18
$\log K_{oct}^b$		1.10	19
P_{vp}^c	torr	0.149 ^d	20
S_w^e	g/cm ³	0.0429 ^f	21
RT (30°C)	Latm/mol	24.89	—
u^g	m/s	1.5	16
Measured or estimated parameters			
h	μm	13.4	5
f	—	0.1	5
k_p^h	cm/h	0.0169	17
$K_{SC/w}^I$		8.71	5

^aDensity.^bOctanol/water partition coefficient.^cVapor pressure.^dExtrapolated from 25°C value of 0.0940 torr by Antoine method.²⁰^eWater solubility.^f25°C value.^gWind velocity.^hSteady-state permeability coefficient from aqueous solution.^IStratum corneum/water partition coefficient for partially hydrated skin (Equation 43 in Reference [5]).

analysis because model parameters were fit to cumulative data rather than flux. There was also a small delay in the evaporation rate profiles for low airflows in the airflow-dependence study (Fig. 4a), as has been previously discussed.^{6,12} We accounted for this delay in the model by adding a correction related to the headspace between the skin surface and the vapor trap. As this feature was of minor consequence for the BA analysis, discussion is deferred to a study in which it plays a larger role.¹¹

At the highest dose (10.6 mg/cm²), the theory predicts a shorter elapsed time for attainment of the maximum absorption rate $t_{abs}(\text{max})$ than was observed experimentally (Fig. 2). In fact, the theoretical flux at this dose is nearly constant from 1.5 to 8 h (data not shown), whereas the experimental flux peaked between 2 and 4 h and fell only slightly during the 4–8 h time period (Tab. 1 and Fig. 1). Thus, the difference in $t_{abs}(\text{max})$ is less substantial than might be inferred by merely studying Figure 2. The key finding was that a prolonged, nearly constant absorption rate was obtained from large doses of BA applied to skin, consistent with the Case 2 scenario in the diffusion model.

Table 5. Derived Diffusion Model Parameters for BA

Parameter	Units	Source	
		Table 3 (Bolded Values)	Table 4
h_{dep}^a	μm	1.50	1.34
k_p^b	cm/h	0.00305 ^c	0.00563 ^d
$D_0 C_{sat}/h$	$\mu\text{g}/\text{cm}^2\text{h}$	131	242
h^2/D_0		2.6	2.07
D_0	cm^2s^{-1}	2.40×10^{-10}	2.41×10^{-10}
C_{sat}	mg/cm ³	227	374
M_{sat}	$\mu\text{g}/\text{cm}^2$	34	50
k_g	cm/h	880	1820 ^e
k_{evap}	cm/h	7.17×10^{-4}	1.49×10^{-3}
χ	—	5.70	6.41

Values were calculated from Equations 2–9 in the text unless otherwise specified.

^aDeposition region.^bSteady-state permeability coefficient for partially hydrated skin.⁵^cCalculated as $(D_0 C_{sat}/h)/S_w$.^dCalculated as $k_p/3$.^eCalculated from Equation 37 in Reference [5].

Independent Estimation of Diffusion Parameters

As noted in the accompanying study⁵ (Evaluation of Parameters section) the parameters associated with the diffusion/evaporation model for an arbitrary permeant can be estimated from existing data and correlations without the need of conducting an experiment. A detailed procedure for this calculation was proposed.⁵ It is instructive to compare the parameters resulting from such a calculation for BA with those arising from the detailed model fitting process described herein. By so doing, one can gain a feel for whether the model in its present form is capable of making useful predictions. Admittedly, this test is for a single compound; however, additional comparisons are possible.^{7,9}

Following the procedure outlined in Reference [5], we first obtained relevant physical properties for BA and selected appropriate environmental conditions. These values are given in Table 4. In order to compare with diffusion cell data obtained in a laboratory fume hood (dose-dependence study), we chose a skin temperature of 30°C and a wind velocity of 1.5 m/s, corresponding to a typical outdoor environment.¹⁶ The four required diffusion model inputs were then estimated as follows: The values $h = 13.4 \mu\text{m}$ and $f = 0.1$ were selected as discussed elsewhere.⁵ The steady-state permeability coefficient for BA in aqueous solution,

Table 6. Percentage Absorption of BA after 24 h Estimated by Three Different Methods

Dose, $\mu\text{g}/\text{cm}^2$	Experimental (Tab. 2)	Diffusion Model Calculations	
		(Tab. 5, Column 3) ^a	(Tab. 5, Column 4) ^b
0.9	19.8 ± 2.9	19.4	17.5
29	21.8 ± 0.9	20.3	17.5
990	25.0 ± 4.7	23.0	13.2
10600	29.2 ± 3.0	23.8	13.1

^aModel estimates obtained by fitting parameters to experimental data (Franz diffusion cells in a fume hood).

^bModel estimates obtained *via* independent parameter estimation method as described in Discussion and Reference [5].

$k_p = 0.0169$ cm/h, was obtained from the literature¹⁷ and an estimate of the corresponding value for partially hydrated skin, $\tilde{k}_p = 0.00563$ cm/h, was made by dividing k_p by three.⁵ An estimate of the SC/water partition coefficient for BA in partially hydrated skin, $\tilde{K}_{\text{SC/w}} = 8.71$, was made using Equation 43 in Reference [5]. The remaining parameters were then calculated from Equations 2–8 or the additional relationships in Reference [5] (Eqs. 36–45). The results of the calculation (Tabs. 5 and 6) are presented in comparison to values obtained using the directly fitted model parameters from Table 3.

Table 5 shows a general agreement between the model parameters obtained *via* the independent parameter estimation method and the experimentally-derived parameters. Although the skin capacity measures M_{sat} and C_{sat} derived by the independent method were 50%–60% larger than those derived experimentally, these differences were offset by higher evaporation rate parameters k_g and k_{evap} , leading to comparable estimates for the dimensionless ratio χ and, hence, of total absorption at low-to-moderate doses (Tab. 6). As dose increased, the independent method under-predicted absorption by a wider margin, since it did not account for increased skin permeability to BA. This effect could be anticipated in a model calculation (e.g., for risk assessment) by building in an appropriate variable diffusivity factor using Equation 10. Thus, we view the comparisons in Tables 5 and 6 as supportive of a predictive capability for the diffusion model. Such a method, according to which transient disposition profiles of either volatile and nonvolatile chemicals on skin could be estimated from physical and environmental properties combined with steady-state permeability data, would have substantial value.

CONCLUSIONS

Many features of the dose and airflow dependence of BA disposition on human skin *in vitro* following solvent deposition have been found to be consistent with a finite dose diffusion model involving evaporative loss from the skin surface and a concentration-dependent diffusivity of BA in the skin. The extent of agreement of these results with independent, model-based estimates of BA skin disposition is supportive of an eventual predictive use of the model.

ACKNOWLEDGMENTS

Financial support for this study was provided by NIOSH/CDC grant R01 OHO7529.

REFERENCES

1. Mookherjee BD, Patel SM, Trenkle RW, Wilson RA. 1998. A novel technology to study the emission of fragrance from the skin. *Perfumer Flavorist* 23: 1–11.
2. Gerberick GF, Robinson MK. 2000. A skin sensitization risk assessment approach for evaluation of new ingredients and products. *Am J Contact Derm* 11:65–73.
3. Basketter DA. 1998. Skin sensitization: Risk assessment. *Int J Cosmet Sci* 20:141–150.
4. Basketter DA, Cookman G, Gerberick GF, Hamaide N, Potokar M. 1997. Skin sensitization thresholds: Determination in predictive models. *Fd Chem Toxic* 35:417–425.
5. Kasting GB, Miller MA. 2005. Kinetics of finite dose absorption through skin 2. Volatile compounds. *J Pharm Sci* 95:268–280.

6. Saiyasombati P, Kasting GB. 2003. Disposition of benzyl alcohol following topical application to human skin in vitro. *J Pharm Sci* 92:2128–2139.
7. Santhanam A, Miller MA, Kasting GB. 2005. Absorption and evaporation of *N,N*-diethyl-*m*-toluamide (DEET) from human skin in vitro. *Toxicol Appl Pharmacol* 204:81–90.
8. Kasting GB, Filloon TG, Francis WR, Meredith MP. 1994. Improving the sensitivity of in vitro skin penetration experiments. *Pharm Res* 11:1747–1754.
9. Santhanam A. 2004. Mathematical model to predict the skin disposition of DEET and other volatile compounds. MS thesis, College of Pharmacy, University of Cincinnati, Cincinnati, OH.
10. Bevington PR. 1969. Data reduction and error analysis for the physical sciences. New York: McGraw-Hill.
11. Bhatt V, Santhanam A, Miller MA, Kasting GB. 2004. Absorption and evaporation of volatile and potentially hazardous chemicals from human skin. Am Assoc Pharm Sci National Meeting, Baltimore, MD.
12. Saiyasombati P, Kasting GB. 2004. Evaporation of benzyl alcohol from human skin in vivo. *J Pharm Sci* 93:515–520.
13. Anissimov YG, Roberts MS. 2001. Diffusion modeling of percutaneous absorption kinetics: 2. Finite vehicle volume and solvent deposited solids. *J Pharm Sci* 90:504–520.
14. Saiyasombati P, Kasting GB. 2003. Two-stage kinetic analysis of fragrance evaporation and absorption from skin. *Int J Cosmet Sci* 25:235–243.
15. Vuilleumier C, Flament I, Sauvegrain P. 1995. Headspace analysis study of evaporation rate of perfume ingredients applied onto skin. *Int J Cosmet Sci* 17:61–76.
16. Peress J. 2003. Estimate evaporative losses from spills. *Chem Eng Prog* 32–34.
17. Johnson ME, Blankschtein D, Langer R. 1997. Evaluation of solute permeation through the stratum corneum: Lateral bilayer diffusion as the primary transport mechanism. *J Pharm Sci* 86:1162–1172.
18. Budavari S. 1996. The Merck Index. Whitehouse Station, NJ: Merck & Co.
19. Hansch C, Leo A. 1999. MEDCHEM database and CLOGP program. Claremont, CA: BioByte, Inc.
20. Meylan W. 1999. MPBPWIN. North Syracuse, NY: Syracuse Research Corporation.
21. Yalkowski SH. 1993. AQUASOL database. University of Arizona, Tucson, AZ.